

## D3.2 Long lived memory with ultracold atoms

MALICIA  
Grant Agreement Number 265522

<b>Project</b>	
Project acronym:	MALICIA
Project full title:	Light-Matter interfaces in absence of cavities
Grant agreement no.:	265522
Funding scheme:	Collaborative Project
Project start date:	01 February 2011
Project duration:	36 months
Call topic:	ICT-2007.8.0 – FET Open
EC project officer:	Matteo Mascagni
Project web-site:	<a href="http://www.maliciaproject.eu/">http://www.maliciaproject.eu/</a>
<b>Document</b>	
Deliverable number:	D3.2
Deliverable title:	<i>Long lived memory with ultracold atoms</i>
Due date of deliverable:	M24
Actual submission date:	M24
Editors:	
Authors:	
Reviewers:	
Participating beneficiaries:	1-LENS; 2-UULM; 5-MPG
Work Package no.:	WP3
Work Package title:	<i>Quantum gases</i>
Work Package leader:	Prof. Francesco Saverio Cataliotti
Work Package participants:	1-LENS; 2-UULM; 5-MPG
Estimated person-months for deliverable:	28
Dissemination level:	PU
Nature:	P
Version:	1
Draft/Final:	Draft
No of pages (including cover):	6
Publishable abstract	
Keywords:	

### D3.2 Long lived memory with ultracold atoms

Cold samples are an ideal medium for studying EIT effects. Indeed, the reduced (almost negligible) Doppler effect allows the exploitation of the intrinsic sharpness of atomic dipole transitions: all the atoms see light at the same frequency and it not necessary to average on a velocity distribution. Moreover, the low mean velocity of the ensemble involves low rates of spatial mixing, and it allows non dissipative trapping. Indeed magnetic trapping, due to its internal state selectivity, provides also a sort of continuous cleanup of the sample, in this environment the probability of recovering in the interaction region an atom lost in a previous moment, which is one of the factors carrying decoherence in warm atoms experiments, is almost null. However implementing a long lived memory with magnetically trapped atoms requires two main precautions:

- 1) the use of a “clock” transition i.e. the transition between  $|F=1, m_F=-1\rangle$  and  $|F=2, m_F=+1\rangle$  sub-states since these two states are shifted by the magnetic field in the same way in linear approximation;
- 2) the use of a “magic” field (around 3.2 Gauss for  $^{87}\text{Rb}$ ) where, taking into account the full Breit-Rabi formula for the magnetic shift of the levels, the differential shift of the two levels is at a minimum.

Until very recently we were unable to work with the above mentioned mixture therefore we report here the results obtained with the transition between  $|F=2, m_F=+2\rangle$  and  $|F=1, m_F=+1\rangle$  states and extrapolate the limits for the optimal choice.

Our Atom Chip at LENS allows the routine realization of condensates of  $^{87}\text{Rb}$  atoms with typically  $5 \cdot 10^4$  atoms. With an atomic density in the range of a few units in  $10^{12}$  atoms  $\text{cm}^{-3}$  this sample would allow optical depths in the excess of 100. However the transverse size of our condensate is of the order of  $2 \mu\text{m}$ . Given the requirement that the optical beam that one wants to store in the sample should be completely contained in the atomic sample this strongly limits the applicability of our magnetically trapped condensate.

Indeed we have chosen to use a trapped cloud of around  $10^7$  atoms at a temperature of  $22 \mu\text{K}$  with a size of  $50 \times 50 \times 220 \mu\text{m}$  so that the transverse dimension of the cloud is larger than our optical beam waist of  $30 \mu\text{m}$ . The expected dephasing is completely dominated by the magnetic field inhomogeneities that we expect to be around 1 MHz. This would be reduced well below the 1 kHz level for the clock transition and the “magic” field. At this point the limiting factor would come from the residual Doppler broadening of around 60 kHz. Atom-atom interactions are negligible in the thermal cloud.

Control and signal field are copropagating beams with opposite polarization. The two beams are merged on a beam splitter before the cell and take opposite  $\sigma$  polarizations crossing a quarter-wave plate. After interacting with the sample, the two fields are separated with a second beam splitter after another quarter-wave plate. To minimize the effect of the almost resonant signal field, we have kept it as weak as necessary to ensure a small damage of the cloud during the measure sequence (few nanowatts). It is detected as beat note with a 5 MHz detuned local oscillator. This

technique allows the detection of such weak fields just with the help of some milliwatts of local oscillator.

The spectroscopy is performed in a discrete way, as a series of control, signal and local oscillator synchronized pulses. While the control field maintains all the time the same one photon detuning, signal and local oscillator change frequency with regular steps at each pulse, keeping the beat note at fixed pulsation. With few nanowatt pulses of length  $4 \mu\text{s}$ , we are able to construct a signal composed of hundreds of pulses of almost resonant light without significantly spoiling the sample.

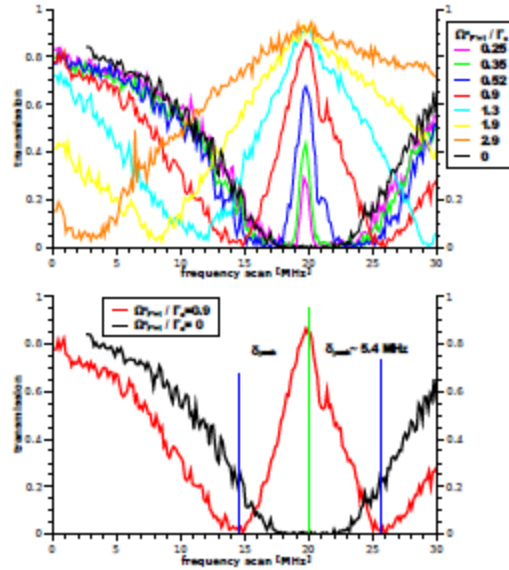


Fig 1: Absorption profiles for a scan of the probe light frequency around the atomic resonance in the presence of one-photon resonant control field. The profiles relative to an increasing control Rabi frequency are reported. The formation of the induced transparency is evident. In the lower panel, one specific case is considered with more attention, the V-like shape shown by the induced transparency profiles is a feature reproducible by simulations accounting for inhomogeneous Zeeman broadening.

We then tried to detect the delay induced by the low group velocity attainable with this sample. Actually the detection procedure is such that it is immediate to switch from spectroscopy-like measurements to temporal profiles detection. While for spectroscopy each segment is demodulated all together, giving the average amplitude value to be confronted with the ones obtained for other segments, here we divide each segment in shorter sub-intervals, which are separately demodulated. In this way we have access to the modulation of the envelope within the temporal window defined by the segment. In the case reported in Fig. 2, for simplicity, we left unchanged the temporal interval of beat note detection ( $4 \mu\text{s}$ ), while providing independent demodulation on sub-intervals of duration  $0.4 \mu\text{s}$ . The temporal profile of the pulses was approximatively Gaussian with a FWHM of  $0.5 \mu\text{s}$  centered on the detection window. In this way each segment contains the whole envelope, and comparing the results for different configurations we can directly explore the variation of delay and absorption.

By providing the same experimental sequence used for the spectroscopy, but maintaining fixed the frequency of all the beams, we are able to ensure a two hundreds set of measurements of the same output pulse profile for a given configuration with a single experimental realization of the cold cloud. Each curve of Fig. 2 is actually the average over such a statistical ensemble.

The temporal resolution in these measurements is limited by the beat note frequency of the spectroscopy experiments (5MHz).

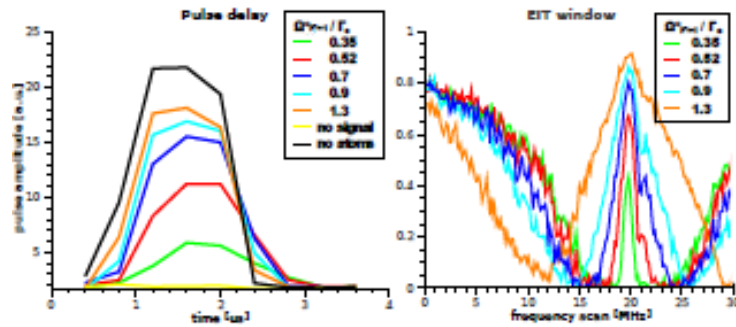


Fig2: Delayed profiles for different control Rabi frequencies. The black curve serves as a reference, it is the pulse profile obtained in the absence of atoms. On the right the EIT spectroscopy signals obtained with the same control Rabi frequencies are reported (colors indicate curves for a given value of the Rabi frequency). The attained delay is low, due to the high decay rate of the hyperfine coherence. Indeed, when approaching control Rabi frequencies able to induce a large delay, the incoherent absorption has already destroyed the pulse.

With these results, we are able to estimate storage times and quantum efficiency.

We have indeed to interpret them considering that the exploited  $\Lambda$  scheme is characterized by a very high coherence decay rate. Using the calibration of the model obtained with our data, we can estimate the results attainable by working with the scheme based on the clock transition. In Fig 3 we show some estimations of delay for such a configuration.

The simulations look very promising, considering also that we have taken into account the less efficient trapping procedure for the clock states by reducing the number of atoms to 75% and weakening the confinement. The improvement is mainly due to the combination of two factors: the reduction of the Raman coherence decay rate by a factor  $1=1000$  with respect to the value used in the experiment, and the larger dipole matrix element corresponding to the transition addressed by the signal field, which is almost twice. The smaller decoherence rate allows to keep a substantial transmission even for lower control Rabi frequency respect to the present case, hence leaving the possibility of exploiting sharper dispersion profiles.

For example, the best result reported in reported in Fig. 3 is obtained for a Rabi frequency which induces a very low transparency in the configuration used for the measurements.

On the other hand, the expression for the susceptibility is proportional to the square of the involved dipole matrix element, thus in the simulated case it has an overall magnification by a factor of 4. The attained coupling with the sample is thus quite satisfactory, and it turns out not too hard to reach day by day.

Concerning the magnetic noise, since its amplitude is of the same order of magnitude of the trapping potential, we conclude that it will not reduce too much the potentialities of the system, which should further improve by approaching the magic bias magnetic field value.

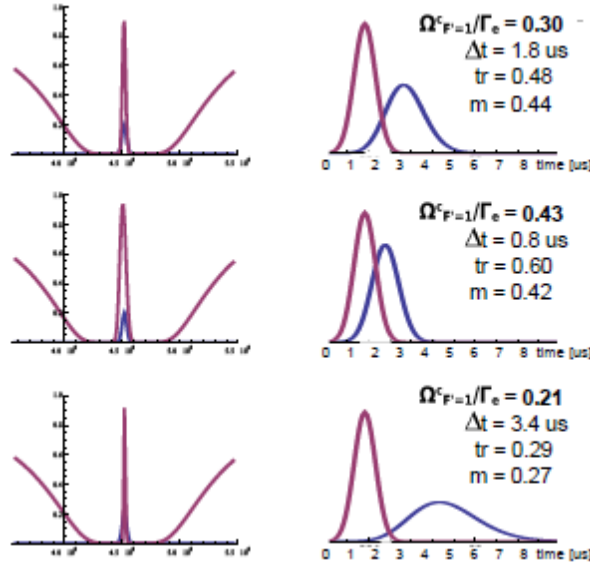


Fig3: Estimation of the attainable time delay  $\Delta t$  and parameter  $m$  by working with the  $\Lambda$  scheme based on the clock transition. This low rate of decoherence allows a substantial transmission of the signal pulse for lower values of the control Rabi frequency with respect to the experimentally explored case, which corresponds to lower group velocities.

At the same time an evaluation of what can be optimized by CRAB techniques has been performed in ULM. As a simple, well controlled example of quantum memory we use an atomic  $\Lambda$ -type system that offers possibility for storage and retrieval of photons.

We have used this relatively simple system to check how much Chopped Random Basis (CRAB) optimization algorithm can increase efficiency and improve fidelity of this process depending on the storage time and a shape of incoming photon wave packet.

The parameters we used for optimization include the time dependent amplitude of the controlling field and detunings from energies of atomic transitions. We worked within a RWA approximation using the Schrodinger picture and incorporating noise/error factors via a Quantum Monte Carlo wave function model, as this way of including dissipation combined with CRAB optimization method allows for efficient numerical calculations.

The system under consideration consists of incoming - outgoing field modes, and an atom with an excited and a long-lived ground state coupled to a classical control field. In the experiment the initial atomic state was coupled to the excited one by the cavity mode, and the overall storage efficiency was determined as 9.3%. In our description the optimization of the control field increases this number to above 20%

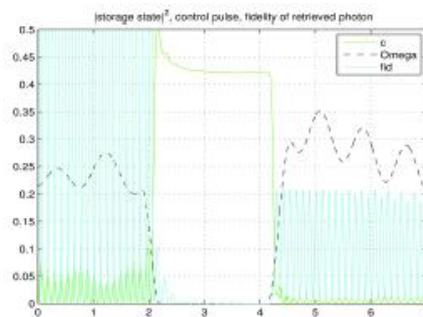


Fig 4: The fidelity of a retrieved photon (blue curve), the envelope of a control field  $\Omega$  (black dashed curve) and the probability of finding a photon in a storage state 'c' (green curve) as a function of time.